

# An Effective Strategy to Tune Supramolecular Interaction via a Spiro-Bridged Spacer in Oligothiophene-*S,S*-dioxides and Their Anomalous Photoluminescent Behavior

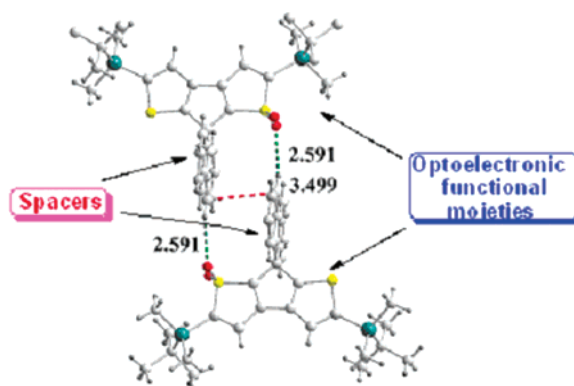
Ling-Hai Xie,<sup>†</sup> Xiao-Ya Hou,<sup>‡</sup> Yu-Ran Hua,<sup>‡</sup> Yan-Qin Huang,<sup>†</sup> Bao-Min Zhao,<sup>‡</sup> Feng Liu,<sup>‡</sup> Bo Peng,<sup>‡</sup> Wei Wei,<sup>‡</sup> and Wei Huang<sup>\*†</sup>

*Institute of Advanced Materials (IAM), Nanjing University of Posts and Telecommunications (NUPT), 66 XinMoFan Road, Nanjing 210003, China, and Institute of Advanced Materials, Fudan University, 220 Handan Road, Shanghai 200433, China*

wei-huang@njupt.edu.cn

Received January 2, 2007

## ABSTRACT



We demonstrate that incorporating nonplanar spiro-bridged structures is an effective strategy for tuning supramolecular interactions of optoelectronic functional moieties. In the model compounds spiro-bridged oligothiophene-*S,S*-dioxides (BSiSDTFO), unusual dimers constructed by spiro-bridged spacers do not form excimers, which is confirmed by crystallographic data and fluorescent emission spectra.

Optoelectronic materials based on  $\pi$ -conjugated organic molecules have attracted much attention due to their applications in organic light-emitting diodes, organic field-effect transistors, nonlinear optics, solar cells, and biosensors, etc.<sup>1</sup> Exploring good candidates for these applications relies on not only the design of molecules at the molecular level but also the elaboration of supramolecular structures because the latter strongly impacts the electronic structures and photophysical

processes in the solid state.<sup>2</sup> For example, the photoluminescence (PL) efficiency of oligothiophene-*S,S*-dioxides in the solid state obviously depends on molecular conformations and supramolecular organizations.<sup>3</sup> In addition, weak supramolecular interactions based on  $\pi$ - $\pi$  stacking is common to many aromatic molecules, under which various supramolecular objects have been formed, such as dimers, excimers, *J*-aggregates, *H*-aggregates, and cross dipole stackings.<sup>4</sup> Thus, one way to further improve the optoelectronic properties of  $\pi$ -conjugated organic molecules is to control supramolecular interactions in the solid state.

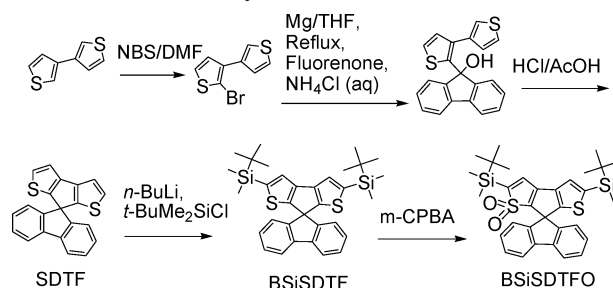
<sup>†</sup> Nanjing University of Posts and Telecommunications (NUPT).

<sup>‡</sup> Fudan University.

Our objective is to utilize rigid geometric factors, e.g., macromolecular disks,<sup>5</sup> helical macromolecules,<sup>6</sup> and cross-shaped spiro structures,<sup>7</sup> to tune supramolecular interactions among optoelectronic functional moieties. Different kinds of geometric conformations could be favorable or unfavorable for the alignment of functional groups by participating in the short intermolecular interactions or acting as spacers. Therefore, incorporating unique rigid geometric conformations into the optoelectronic groups is a very good approach to explore novel optoelectronic materials with high performance. In this communication, we demonstrate that incorporating nonplanar spiro-bridged frameworks into thiophene-*S,S*-dioxides is an effective way to tune supramolecular interactions of oligothiophene-*S,S*-dioxide chromophores. Some unusual dimers constructed by spiro-bridged spacers do not form excimers, which were confirmed by crystallographic data and fluorescent emission spectra. The weak intermolecular supramolecular interactions among thiophene-*S,S*-dioxides were greatly depressed due to the existence of biphenyl moieties as an “insulated spacer”, which is beneficial to the fluorescent quantum efficiency in the solid state.

The synthetic route of model compound BSiSDTFO is outlined in Scheme 1. The spirodithiophene-fluorene (SDTF) was prepared following the synthetic route of spirobifluorene. Addition of the 3,3-bithienyl Grignard reagent to fluorenone gave the tertiary alcohol, followed by Friedel–Crafts dehydration cyclization in a mixture of hydrochloride and acetic acid to obtain SDTF in an almost quantitative yield. BSiSDTF was easily obtained by 2 equiv of *n*-BuLi with SDTF followed by quenching the Me<sub>2</sub>-*t*-BuSiCl reagent. BSiSDTF was oxidized at the thienyl sulfurs by *m*-CPBA to afford stable mono-*S,S*-dioxides BSiSDTFO in 60% yield.<sup>8</sup>

**Scheme 1.** Synthetic Route to BSiSDTFO



However, spiro-bridged bis-*S,S*-dioxides were still not obtained, although largely excessive *m*-CPBA was attempted.

The structure of BSiSDTFO was confirmed by <sup>1</sup>H and <sup>13</sup>C NMR, MALDI-TOF MS, elemental analysis, and single-crystal X-ray diffraction. Single crystals of BSiSDTF and BSiSDTFO were obtained from a CH<sub>2</sub>Cl<sub>2</sub>/alcohol solution.<sup>9</sup> There is a slight lengthening of the C–S bond next to the oxygen atom in BSiSDTFO (from mean values of 1.740 and 1.703 in BSiSDTF to 1.772 and 1.744 in BSiSDTFO), which implies loss of the aromatic conjugation due to oxidation of the sulfur atom. Various short intermolecular contacts participate in the molecular packing of BSiSDTFO, including C–H···O, C–H···S, and C–H···π hydrogen bonds and π–π stacking (Figure 1). The typical C–H···O distance of 2.591 Å is consistent with 2.57 Å, which was observed in the rigid-core oligothiophene dioxides.<sup>10</sup> However, no extremely short S···O and S···S separations in BSiSDTFO were observed, which are the main driving forces to promote self-assembled three-dimensional networks in planar oligothiophene-*S,S*-dioxides.<sup>11</sup> Therefore, it is natural to conclude that spiro frameworks play an important role in interrupting the supramolecular interactions between S and O atoms or S and S atoms that lead to the formation of excimer emission and the increase of the self-quenching probability in the solid state.

(1) (a) Skotheim, T. A.; Elsenbaumer, R. L.; Reynolds, J. R. *Handbook of Conducting Polymers*; Marcel Dekker Inc.: New York, 1998. (b) Facchetti, A.; Yoon, M.-H.; Stern, C. L.; Katz, H. E.; Marks, T. J. *Angew. Chem., Int. Ed.* **2003**, *42*, 3900–3903. (c) Mazzeo, M.; Vitale, V.; Sala, F. D.; Pisignano, D.; Anni, M.; Barbarella, G.; Favaretto, L.; Zaneli, A.; Cingolani, R.; Gigli, G. *Adv. Mater.* **2003**, *15*, 2060–2063. (d) Pisignano, D.; Anni, M.; Gigli, G.; Cingolani, R.; Zavelani-Rossi, M.; Lanzani, G.; Barbarella, G.; Favaretto, L. *Appl. Phys. Lett.* **2002**, *81*, 3534–3536. (e) Barbarella, G.; Zambianchi, M.; Pudova, O.; Paladini, V.; Ventola, A.; Cipriani, F.; Gigli, G.; Cingolani, R.; Citro, G. *J. Am. Chem. Soc.* **2001**, *123*, 11600–11607. (f) Barbarella, G. *Chem.–Eur. J.* **2002**, *8*, 5072–5077. (g) Sotgiu, G.; Zambianchi, M.; Barbarella, G.; Aruffo, F.; Cipriani, F.; Ventola, A. *J. Org. Chem.* **2003**, *68*, 1512–1520.

(2) (a) Fratiloiu, S.; Senthilkumar, K.; Grozema, F. C.; Christian-Pandya, H.; Niazimbetova, Z. I.; Bhandari, Y. J.; Galvin, M. E.; Siebbeles, L. D. A. *Chem. Mater.* **2006**, *18* (8), 2118–2129. (b) Drummy, L. F.; Miska, P. K.; Alberts, D.; Lee, N.; Martin, D. C. *J. Phys. Chem. B* **2006**, *110* (12), 6066–6071. (c) Terenziani, F.; Mongin, O.; Katan, C.; Bhatthula, B. K. G.; Blanchard-Desce, M. *Chem.–Eur. J.* **2006**, *12*, 3089–3102.

(3) Barbarella, G.; Favaretto, L.; Sotgiu, G.; Zambianchi, M.; Bongini, A.; Arbizzani, C.; Mastragostino, M.; Anni, M.; Gigli, G.; Cingolani, R. *J. Am. Chem. Soc.* **2000**, *122* (48), 11971–11978.

(4) Xie, Z.; Yang, B.; Li, F.; Cheng, G.; Liu, L.; Yang, G.; Xu, H.; Ye, L.; Hanif, M.; Liu, S.; Ma, D.; Ma, Y. *J. Am. Chem. Soc.* **2005**, *127* (41), 14152–14153.

(5) Fechtenkötter, A.; Tchegobareva, N.; Watson, M.; Müllen, K. *Tetrahedron* **2001**, *57*, 3769–3783.

(6) (a) Marsella, M. J.; Kim, I. T.; Tham, F. *J. Am. Chem. Soc.* **2000**, *122*, 974–975. (b) Iwasaki, T.; Kohinata, Y.; Nishide, H. *Org. Lett.* **2005**, *7*, 755–758.

(7) Xie, L.-H.; Hou, X.-Y.; Tang, C.; Hua, Y.-R.; Wang, R.-J.; Chen, R.-F.; Fan, Q.-L.; Wang, L.-H.; Wei, W.; Peng, B.; Huang, W. *Org. Lett.* **2006**, *8*, 1363–1366.

(8) Barbarella, G.; Pudova, O.; Arbizzani, C.; Mastragostino, M.; Bongini, A. *J. Org. Chem.* **1998**, *63*, 1742–1745.

(9) Data for X-ray structure analysis were collected at room temperature on a Bruker SMART 1K CCD area detector with graphite-monochromated Mo K $\alpha$  radiation ( $\lambda = 0.71073$  Å). The absorption correction was applied by integration based on the crystal shape. Structures were solved by direct methods and refined against F<sup>2</sup> with the full-matrix, least-squares methods using SHELXS-97 and SHELXL-97, respectively. Hydrogen atoms were found by difference Fourier syntheses and were refined. Crystal data for BSiSDTF: C<sub>33</sub>H<sub>40</sub>S<sub>2</sub>Si<sub>2</sub>, *M* = 556.95, colorless cuboid 0.35 × 0.20 × 0.20 mm, monoclinic, *P*<sub>2</sub><sub>1</sub>/*c*, *Z* = 8, *a* = 25.681(11) Å, *b* = 12.073(5) Å, *c* = 23.725(10) Å,  $\alpha = 90^\circ$ ,  $\beta = 117.111^\circ(5)$ ,  $\gamma = 90^\circ$ , *V* = 6547(5) Å<sup>3</sup>, *F*(000) = 2384,  $\rho_{\text{calcd}} = 1.130$  Mg m<sup>-3</sup>,  $\mu$  (Mo K $\alpha$ ) = 0.255 mm<sup>-1</sup>,  $2\theta_{\text{max}} = 50.02^\circ$ , reflections collected/unique 29 035/11 504 (*R*<sub>int</sub> = 0.0331), parameters 667, final *R*1 = 0.0636 (*I* > 2 $\sigma$ (*I*)), *wR*2 = 0.1241 (all data), *S* = 1.018 (all data). Crystal data for BSiSDTFO: C<sub>33</sub>H<sub>40</sub>O<sub>2</sub>S<sub>2</sub>Si<sub>2</sub>, *M* = 588.95, green needle 0.15 × 0.10 × 0.02 mm, triclinic, *P*1, *Z* = 4, *a* = 12.45(4), *b* = 12.94(4), *c* = 22.63(7) Å,  $\alpha = 80.74^\circ$  (3),  $\beta = 86.74^\circ$  (5),  $\gamma = 79.99^\circ$  (6), *V* = 3543 (18) Å<sup>3</sup>, *F*(000) = 1256,  $\rho_{\text{calcd}} = 1.104$  Mg m<sup>-3</sup>,  $\mu$  (Mo K $\alpha$ ) = 0.243 mm<sup>-1</sup>,  $2\theta_{\text{max}} = 50.02^\circ$ , reflections collected/unique 16 005/12 289 (*R*<sub>int</sub> = 0.1938), parameters 703, final *R*1 = 0.2879 (*I* > 2 $\sigma$ (*I*)), *wR*2 = 0.2273 (all data), *S* = 0.556 (all data). CCDC 617286 and 617287 contain the supplementary crystallographic data for this paper. These data can be obtained free of charge from The Cambridge Crystallographic Data Centre via www.ccdc.cam.ac.uk/data\_request/cif.

(10) Tedesco, E.; Sala, F. D.; Favaretto, L.; Barbarella, G.; Albesa-Jove, D.; Pisignano, D.; Gigli, G.; Cingolani, R.; Harris, K. D. M. *J. Am. Chem. Soc.* **2003**, *125* (40), 12277–12283.

(11) Barbarella, G.; Favaretto, L.; Sotgiu, G.; Antolini, L.; Gigli, G.; Cingolani, R.; Bongini, A. *Chem. Mater.* **2001**, *13*, 4112–4122.

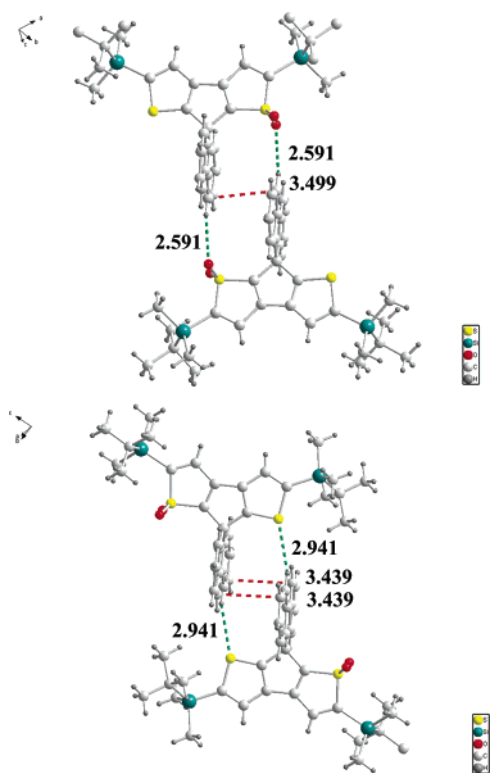


**Figure 1.** Two types of dimeric arrangements within BSiSDTFO molecule crystals through  $\pi$ - $\pi$  stacking of the antiparallel interactions of two fluorene planes and C-H $\cdots$ O/C-H $\cdots$ S hydrogen bonding of intermolecular interactions.

Despite the fact that thienyl sulfur and the sulfonic oxygen of BSiSDTFO are involved in many short intermolecular contacts up to 12 types, most of the short contacts occur between the carbon of fluorene and the thienyl oxygen or sulfur instead of among the chromophores of thiophene-*S,S*-dioxides. In addition, crystallographic data show that BSiSDTFO has two different types of recognizable “dimers” with antiparallel head-to-tail stacking of fluorene ring interaction planes, in which three-dimensional organization is achieved through one face-to-face  $\pi$ - $\pi$  stacking intermolecular interaction with distances of 3.499 and 3.439 Å, respectively, and two pairs of C-H $\cdots$ O or C-H $\cdots$ S intermolecular interactions (Figure 1). The above X-ray results indicate that the spiro-type spacers render the molecular structure extremely bulky compared to the planar structures, which not only increases the molecular rigidity but also hinders close packing and intermolecular interaction of chromophores. Consequently, the introduction of a spiro-type linkage into thienyl-*S,S*-dioxides probably is favorable for the improvement of the luminescent quantum yields in the crystallization state.

The absorption and PL spectra of BSiSDTFO in  $10^{-5}$  M solutions of nonpolar cyclohexane and highly polar  $\text{CHCl}_3$  and in the solid film are shown in Figure 2. The absorption spectrum of BSiSDTFO is comprised of two peaks at ca. 258 and ca. 310 nm and a weak and broad band at ca. 400 nm in both solvents. The band at ca. 400 nm, which can be

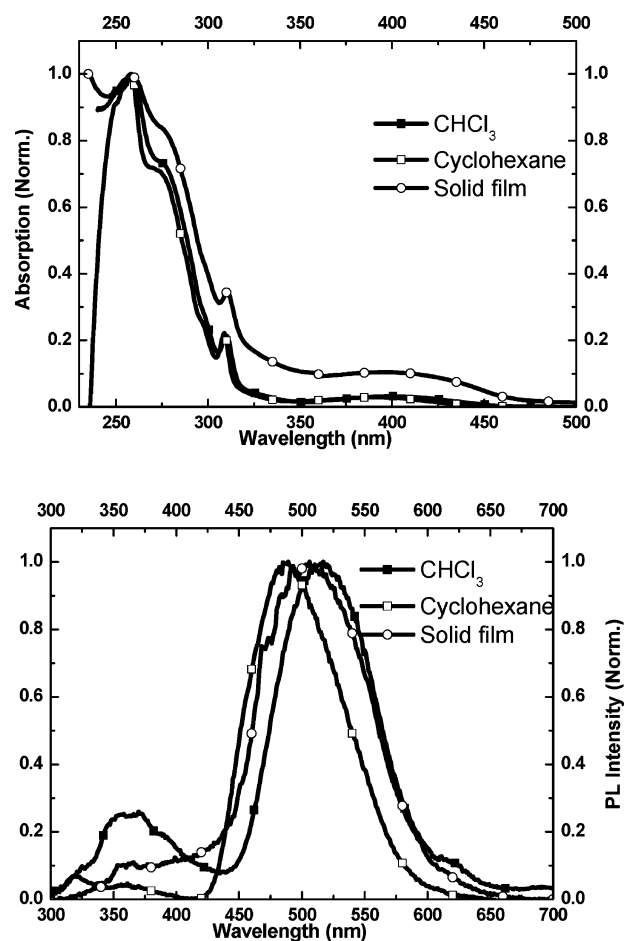


**Figure 2.** UV and PL spectra of BSiSDTFO in cyclohexane,  $\text{CHCl}_3$ , and a solid film.

ascribed to HOMO–LUMO charge-transfer excitation, has a positive solvatochromic shift (red shifts) with increasing solvent polarity, indicating higher polarity exists in the excited state than in the ground state. On selective excitation of 310 nm, the PL emission spectrum of BSiSDTFO in cyclohexane shows a green emission band with a maximum at 488 nm. However, the PL maximum emission of BSiSDTFO in  $\text{CHCl}_3$  is red shifted by 27–515 nm, indicating a strong polar character of the excited-state species in the presence of the thiophene-*S,S*-dioxide. Compared with that in solution, the PL maximum emission in the solid film has a red shift of less than 15 nm, which indicates that no excimer was formed although two recognizable dimers were found in crystal analyses. It is worth mentioning that the emission is originally from energy transfer because the band at ca. 370 nm can always be found in nonpolar cyclohexane, strongly polar  $\text{CHCl}_3$ , and the solid film. In addition, BSiSDTFO exhibits much higher quantum efficiency in the solid state (ca. 20%) than that in the  $\text{CHCl}_3$  solution (3%).

Quantum chemical calculations based on ab initio B3LYP/6-31G\* gave the electronic densities and energies of the HOMO and LUMO frontier orbitals of BSiSDTFO. The lowest singlet excited state of BSiSDTFO is mainly localized

on the oxygenated moieties, whereas the LUMO of the corresponding BSiSDTF is more dispersed along the entire aromatic backbone of fluorene.

For comparison, the cyclic voltammograms (CVs) of BSiSDTFO together with BSiSDTF in the oxidation and reduction domains are provided in Figure 3. The HOMO

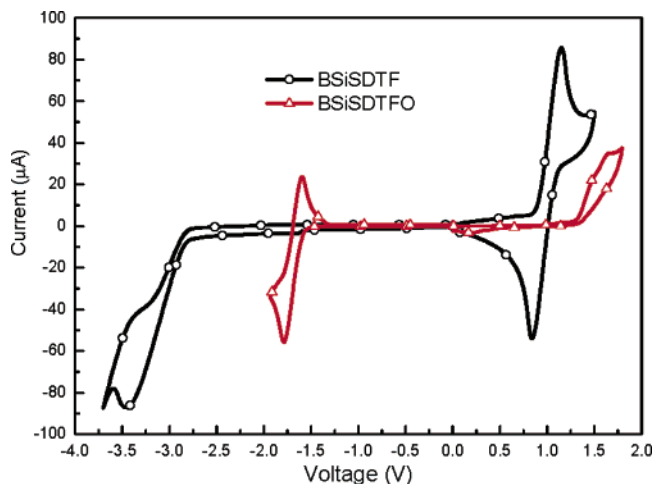


**Figure 3.** Cyclic voltammograms of BSiSDTFO and precursor BSiSDTF measured at a scan rate of 100 mV/s.

and LUMO levels were estimated on the basis of an oxidation potential of  $-4.8$  eV (below the vacuum level) for the ferrocene/ferrocenium ( $\text{Fc}/\text{Fc}^+$ ). The onset potentials of oxidation and reduction for BSiSDTFO were determined to be 1.25 and  $-1.51$  V, respectively (vs  $\text{Ag}/\text{Ag}^+$ ). Thus, HOMO and LUMO energy levels were estimated to be  $-6.00$  and  $-3.24$  eV, respectively (Table 1). The oxidation potential of BSiSDTFO increases only by 0.42 V with respect to that of parent BSiSDTF, and the reduction potential is shifted by 1.25 V toward less negative values, resulting in a substantial increase of the electron affinity and also a decrease of the energy gap of BSiSDTFO with respect to DiSiSDTF. The results clearly reveal that the presence of *S,S*-dioxides has a drastic effect on the reduction process,

**Table 1.** Electrochemical Properties of BSiSDTF and BSiSDTFO<sup>a,b</sup>

compound	$E_{\text{onset}}^{\text{ox}}$ (V)	$E_{\text{onset}}^{\text{red}}$ (V)	HOMO (eV)	LUMO (eV)	$E_g$ (eV)
BSiSDTF	0.83	$-2.76$	$-5.68$	$-1.99$	3.59
BSiSDTFO	1.25	$-1.51$	$-6.00$	$-3.24$	2.76

<sup>a</sup> Determined from cyclic voltammetry in  $\text{CH}_2\text{Cl}_2$  for oxidation potentials and in THF for reduction potentials (0.1 M  $n\text{-Bu}_4\text{N}^+\text{PF}_6^-$  as a supporting electrolyte) using  $\text{Ag}/\text{Ag}^+$  (0.01 M) as a reference electrode at a scan rate of 100 mV/s. <sup>b</sup>HOMO and LUMO levels were determined using the following equations:  $\text{HOMO/LUMO} = -e(E_{\text{onset}} - 0.0468 \text{ V}) - 4.8$  eV, where the value 0.0468 V is for FOC vs  $\text{Ag}/\text{Ag}^+$ .

i.e., on the electron affinity, and a much smaller effect on the oxidation process, i.e., on the ionization potential.

In conclusion, a strategy to control the supramolecular interaction among chromophores has initially been developed by incorporating spiro-bridged frameworks into oligothiophene-*S,S*-dioxides, which has been confirmed by a single-crystal X-ray diffraction study. Recognizable dimers instead of excimers can be deduced from the combination of crystallographic data analysis and optical spectra, which is probably favorable for photoluminescence in the solid state. The improved electron affinity indicates that spiro-bridged oligothiophene-*S,S*-dioxides are potential electron-transporting and hole-blocking materials with high performance.

**Acknowledgment.** This work was financially supported by the NNSFC under Grants 60235412, 90406021, 50428303, and 20574012 and by Nanjing University of Posts and Telecommunications under Grant NY206072. L.-H.X. appreciates the technical support of Ms Ran Sun with Nanjing University.

**Supporting Information Available:** The experimental procedures for the new compounds,  $^1\text{H}$  NMR,  $^{13}\text{C}$  NMR, and MS spectra, and a molecular packing graph. This material is available free of charge via the Internet at <http://pubs.acs.org>.

OL070006U